

ANALYSIS OF TIME SERIES OF POLARIMETRIC SEA ICE SIGNATURES OBSERVED IN FAST ICE IN THE BELGICA BANK AREA

Torbjørn Eltoft¹, Malin Johansson¹, Johannes Lohse¹, Laurent Ferro-Famil²

¹ UiT the Arctic University of Norway, ² Institut Supérieur de l'Aéronautique et de l'Espace, France

1. ABSTRACT

The CIRFA-Cruise 2022 with *RV Kronprins Haakon* to the north-eastern coast of Greenland in the period April 22nd to May 9th 2022 was organised to perform measurements and make observations which allow for validation of sea ice remote sensing information and forecast products resulting from work in the Centre for Integrated Remote Sensing and Forecasting for Arctic Operations (CIRFA), a Centre for Research-based Innovation at UiT the Arctic University of Norway. This paper uses data collected during the cruise to investigate questions related to the interpretation and temporal consistency of polarimetric features computed from a series of quad-pol Radarsat-2 (RS-2) images, which was collected over a fast ice site in the Belgica Bank area in the western Fram Strait. The CIRFA-2022 Cruise team visited this fast ice site in the end of April 2022. The time series covers the transition from cold winter conditions in April to melting in mid June. This transition impacts radar backscattering, as can be clearly seen in the Pauli decomposition of quad-pol images.

Index Terms— SAR, Radar polarimetry, Sea ice

2. INTRODUCTION

Sea ice is known to be an inhomogeneous medium composed of ice, with inclusions of air bubbles, brine channels and solid salt. It can be divided broadly into three categories by age; young ice, which is typically less than 30 cm thick, first-year ice (FYI), and multi-year ice (MYI) [1]. FYI consists of a primary layer of frazil, followed by a much thicker layer of vertically oriented columnar crystals. Its salinity varies with depth, with up to 16 ppt at the top, less in the middle, and then up to 30 ppt at the bottom. Its density varies between 0.90-0.96 g/cm³. The upper surface may be smooth or rough, depending on the prevailing weather conditions during the ice formation. MYI has undergone a process of recrystallisation during the summer melt cycle. The upper surface is

rough, consisting of refrozen melt-ponds and hummocks. The density varies with depth, with lighter ice at the top (typically 0.70 g/cm³), and heavier ice at the bottom (0.90 g/cm³). The salinity is low, i.e. less than 3 ppt [1].

Electromagnetic (EM) wave propagation and scattering in sea ice is determined by the permeabilities and permittivities of its constituents, their fractional composition, and geometrical relationships and orientations. EM properties are further complicated by being dependent on physical properties of the surface, such as small-scale roughness, degree of large-scale deformation, and snow cover. A sea ice surface with a layered snow cover is a multilayered medium, where the backscattered C-band radar signal in general will have contributions from both surface and volume scattering processes. It is well-known that SAR polarimetry can reveal scattering mechanisms and physical characteristics of the target surface. Polarimetric signatures of sea ice will vary with ice type and the properties of possible snow on top of it. Many research papers published during the last couple of decades have reported about the advantages of SAR polarimetry for sea ice classification, but there still are uncertainties as to the interpretation of polarimetric signatures of sea ice and how these signatures relate to the physical properties of the ice [2], [3],[4],[5]. Furthermore, there are open questions related to the temporal stability of these features, and how they vary with changes in meteorological conditions. In this brief paper, we present some preliminary results of a polarimetric analysis of a time series of quad-pol RS-2 images collected over a fast ice site at the north-eastern coast of Greenland in the period April - June, 2023.

3. ANALYSIS

The data analysed consists of a set of 11 RS-2 scenes collected over fast ice in Belgica Bank in the period April 11th to June 18th, 2022. The images were acquired at incidence angles ranging from 30 to 44 degrees, and cover several types of snow-covered sea ice areas, including level FYI, deformed MYI, and thin young ice in refrozen leads. During the first part of the time period, the area had cold winter conditions, with a dry snow cover. The temperatures gradually increased through the last part of May, and towards the end of the data collection, the site area experienced warm temperatures and

The CIRFA-2022 Cruise and the current work was funded by UiT the Arctic University of Norway, the Centre for Integrated Remote Sensing and Forecasting for Arctic Operations (CIRFA) under the Research Council of Norway Grant no. 237906, and the CIRFAEx project under ESA Contract No. 4000139879/22.

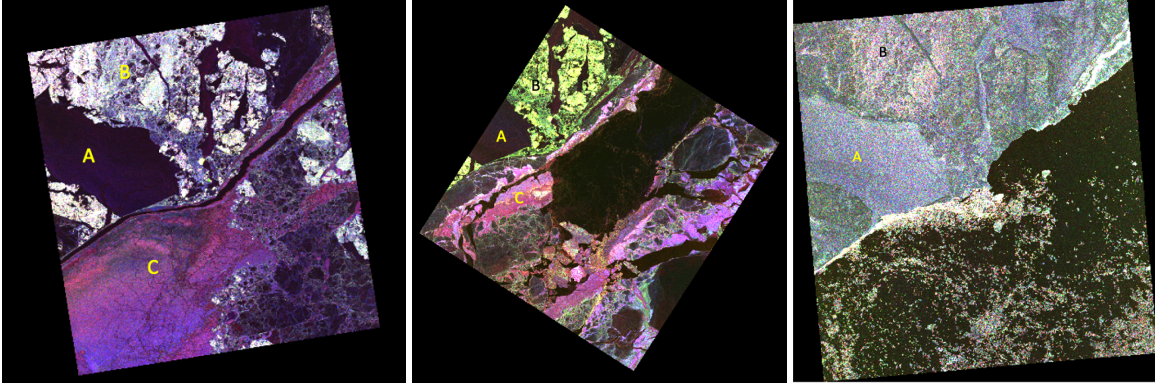


Fig. 1. Pauli images of RS-2 images from April 11, May 4, and June 18.

melting conditions. In the current paper, we will use changes in the visual appearance of the polarimetric Pauli image to monitor variations in scattering mechanisms.

The Pauli image is a kind of coherent target decomposition. It expresses the measured scattering matrix S in the so-called Pauli basis. In the 3-dimensional Pauli representation, the scattering vector is, under the reciprocity assumption, defined as

$$\mathbf{k}_P = \frac{1}{\sqrt{2}} [s_{hh} + s_{vv}, s_{hh} - s_{vv}, 2s_{hv}], \quad (1)$$

where the square-root factor is used to keep the total backscattered power constant. The measured scattering matrix is then expressed as

$$\mathbf{S} = \alpha \mathbf{S}_s + \beta \mathbf{S}_d + \gamma \mathbf{S}_v, \quad (2)$$

where

$$\mathbf{S}_s = \frac{1}{\sqrt{2}} \begin{bmatrix} 1 & 0 \\ 0 & 1 \end{bmatrix}, \quad \mathbf{S}_d = \frac{1}{\sqrt{2}} \begin{bmatrix} 1 & 0 \\ 0 & -1 \end{bmatrix}, \quad (3)$$

$$\mathbf{S}_v = \frac{1}{\sqrt{2}} \begin{bmatrix} 0 & 1 \\ 1 & 0 \end{bmatrix},$$

and

$$\alpha = \frac{S_{HH} + S_{VV}}{\sqrt{2}}, \quad \beta = \frac{S_{HH} - S_{VV}}{\sqrt{2}}, \quad \gamma = \frac{2S_{HV}}{\sqrt{2}}. \quad (4)$$

$|\alpha|^2$, $|\beta|^2$, and $|\gamma|^2$ represent the scattering power associated with surface, double bounce, and volume scattering, respectively [6]. Figure 1 illustrates how the colour of the Pauli images of the RS-2 acquisitions changes from April 11 (left) to May 4 (middle) to June 18 (right). The areas marked as A, B and C in the images correspond to level FYI, deformed MYI, and young lead ice, respectively. The area marked as A, is displayed dark in the two leftmost images, reflecting very low backscatter, for all scattering mechanisms. In-situ measurements confirmed that this area was basically smooth, level first year ice. Area B in the left-hand image, displayed in

a bluish/purplish colour, is verified to be thin young ice. This ice is drifting, and ice area undergoes big changes within the timespan of the time series. Also seen in the left image, the area C, which is deformed ice, is displayed white, indicating strong contributions from all three scattering mechanisms. In the middle image, this region has a strong greenish colour, indicating strong volume scattering. We think this is related to changes in the snow on the ice floe due to the diurnal temperature cycle. This day, the day temperature had risen from around -15^0 to -1^0 C. In the image from June 18, the lead ice has disappeared. We are now well into the melting season, which is clearly seen from the dramatic change in the Pauli colouring of the sea ice scene to the right. The overall colour tone is greenish. The area A appears brighter, with a bluish colour, reflecting more dominant surface scattering. The surface scattering is thought to be attributed to changes in the snow, which presumably has become more wet.

4. CONCLUSION

In this extended abstract, we have combined a time series of quad pol SAR images with in-situ information collected during the CIRFA-2022 cruise in April/May 2022 to study the interpretability of polarimetric parameters over sea ice. We illustrated in this short note how the colours of three associated Pauli images changes in the transition from cold winter conditions to melting temperatures. This indicates changes in the dominant scattering mechanisms, most probably related to snow-related effects. More results of the analysis will be shown at IGARSS-2023, and in future publications.

5. REFERENCES

- [1] M. R. Vant, R. O. Ramseier, and V. Makios, "The complex-dielectric constant of sea ice at frequencies in the range 0.1-40 Ghz," *Journal of Applied Physics*, vol. 49, no. 8, pp. 1264–1280, 1978.

- [2] S. V. Nghiem, R. Kwok, S. H. Yueh, and M. R. Drinkwater, "Polarimetric signatures of sea ice. 2. experimental observations," *Journal of Geophysical Research*, vol. 100, no. C7, pp. 13 681–13 698, 1995.
- [3] J. P. S. Gill and J. J. Yackel, "Evaluation of c-band sar polarimetric parameters for discrimination of first-year sea ice types," *Can. J. Remote Sensing*, vol. 38, no. 3, pp. 306–323, 2012.
- [4] M.-A. Moen, S. N. Anfinsen, A. P. Doulgeris, A. H. H. Renner, and S. Gerland, "Assessing polarimetric sar sea-ice classifications using consecutive day images," *Annals of Glaciology*, vol. 56, no. 69, pp. 285–294, 2015.
- [5] M. Shokr and M. Dabboor, "Observations of sar polarimetric parameters of lake and fast sea ice during the early growth phase,," *Remote Sensing of Environment*, vol. 247, no. 9, pp. 111 910 – 111 920, 2020.
- [6] J.-S. Lee and E. Pottier, *Polarimetric Radar Imaging: From Basics to Applications*, ser. Optical Science and Engineering. Boca Raton, USA: CRC Press, 2009, no. 143.